

Identifying Crop Leaf Angle Distribution Based on Two-Temporal and Bidirectional Canopy Reflectance

Wenjiang Huang, Zheng Niu, Jihua Wang, Liangyun Liu, Chunjiang Zhao, and Qiang Liu

Abstract—The effect of crop leaf angle on the canopy-reflected spectrum cannot be ignored in the inversion of leaf area index (LAI) and the monitoring of the crop-growth condition using remote-sensing technology. In this paper, experiments on winter wheat (*Triticum aestivum* L.) were conducted to identify the crop leaf angle distribution (LAD) by two-temporal (erecting and elongation stages) and bidirectional *in situ* reflected spectrum and the Airborne Multiangle Thermal Infrared (TIR) Visible Near-Infrared (VNIR) Imaging System (AMTIS) images. The distribution characters of the leaf angle for different LAD varieties were expressed using the beta-distribution function and the SAILTH radiative transfer models. The proportion of the leaf angle in 5° angle classes (from 5° to 90°) for erectophile, planophile, and horizontal varieties was dominated by 75°, 55°, and 35°. The different LAD varieties had a similar canopy reflectance in 680 nm (red) and 800 nm (near-infrared band) at the erecting stage, while they had significant differences at the elongation stage. The ratio of the canopy reflectance of 800 nm at the erecting stage [R800(B)] to the canopy reflectance of 800 nm at the elongation stage [R800(A)] was used to identify the different LAD varieties through the selected two-temporal canopy reflectance. A method based on the semiempirical model of the bidirectional reflectance distribution function (BRDF) was also introduced in this paper. The structural parameter-sensitive index (SPEI) was used in this paper for crop LAD identification. SPEI is proved to be more sensitive to identify erectophile, planophile, and horizontal LAD varieties than the structural scattering index and the normalized difference f-index. We found that it is feasible to identify horizontal, planophile, and erectophile LAD varieties of wheat by studying two-temporal and bidirectional canopy-reflected spectrum.

Index Terms—Bidirectional reflectance distribution function (BRDF), identification, leaf-angle distribution (LAD), two-temporal, winter wheat.

Manuscript received March 27, 2006; revised June 12, 2006. This work was supported in part by the Knowledge Innovation Program of the Chinese Academy of Sciences (KZCX3-SW-338), the National Natural Science Foundation (40571117, 40471093, 40571118, and 40401042), the Beijing Natural Science Foundation (4052014), the Special Funds for Major State Basic Research Project (2005CB121103), and the China Postdoctoral Science Foundation (20060390095 and 2006-G63).

W. Huang is with State Key Laboratory of Remote Sensing Science, Jointly sponsored by the Institute of Remote Sensing Applications of the Chinese Academy of Sciences and Beijing Normal University, Beijing 100101, China, and also with the National Engineering Research Center for Information Technology in Agriculture, Beijing 100097, China (e-mail: yellowstar0618@163.com; huangwj@nercita.org.cn).

Z. Niu and Q. Liu are with the State Key Laboratory of Remote Sensing Science, Jointly sponsored by the Institute of Remote Sensing Applications of the Chinese Academy of Sciences and Beijing Normal University, Beijing 100101, China.

J. Wang, L. Liu, and C. Zhao are with the National Engineering Research Center for Information Technology in Agriculture, Beijing 100097, China.

Digital Object Identifier 10.1109/TGRS.2006.881755

I. INTRODUCTION

REMOTE SENSING is a valuable tool for mapping and quantifying field biophysical variations for the application in research and management [19]. Leaf size and angle vary widely across species [5]. Leaf angle affects light interception [7], [11], [28], which influences canopy reflectance [22], [27]. Mickelson *et al.* [18] suggested a number of heritable traits including leaf number, leaf angle distribution (LAD), and tassel size to determine heritable differences among genotypes for light interception. The crop LAD should then be taken into consideration by using remote-sensing techniques to monitor crop-growth status. The relationship between the canopy geometry and the reflectance has been the focus of a great deal of research (e.g., [9], [16], [23], and [33]). Pepper *et al.* [21] concluded that the leaf-orientation-distribution value (LOV) could indicate the leaf-inclination angle and the position where the leaf began to incline. According to this, the degree of leaf inclination could be determined. A research on extracting crop LAD has been performed by Bonhomme *et al.* [3] with canopy radiation absorption pattern, and by Li and Wang [14] using a computed tomography approach.

However, for large-scale crop identification of LAD, a method based on canopy reflectance would be ideal. Many techniques tried to improve the accuracy of land surface parameter retrievals from satellite data using the spectral, angular, and temporal information content of the LAD data. Among these techniques, the angular domain technique has attracted more attention because it can provide a rich information source. The bidirectional reflectance distribution function (BRDF) model establishes the relationship between the bidirectional reflectance and the LAD features of the crop, such that the BRDF is determined by specifying the necessary parameters of the cover type, the viewing, and illumination geometries. Sandmeier *et al.* [26] proposed the anisotropy factor (ANIF) and anisotropy index (ANIX), which are based on reflectance ratios at different viewing or illumination geometries. They found obvious differences between an erectophile grass lawn and a planophile watercress canopy. The parameters of physical BRDF models are related to the canopy biophysical structural information. Gao *et al.* [6] proposed a structural scattering index (SSI) and a relative SSI (RSSI), which were derived from the BRDF parameters. The SSI and RSSI indexes showed that they had both theoretical and practical meaning, and they could be used to distinguish or to detect different land cover types.

With the development of remote-sensing techniques, two-temporal and bidirectional spectral data are being applied in

crop management. Temporal remote-sensing data alone can be used to detect crop status at a given stage, while two-temporal data can explain the dynamic change of crops and monitor land-cover changes [10], [29]. Bidirectional reflectance can be used for crop geometry identification. However, the complexity of canopy geometry and other external factors limit the application of remote-sensing techniques in LAD identification. Li and Wang [15] and Yan *et al.* [31] pointed out that the vegetation canopy geometry has great effects on developing vegetation optical models. To improve the inversion accuracy of crop biochemical and biophysical content, previous knowledge from the ground is needed. In other words, the spectral data, crop LAD, and other previous knowledge should be obtained as much as possible when remote sensing is used to guide crop management. Therefore, it is important to obtain the information of different LAD varieties at the early growth stage to improve the estimation accuracy of crop-growth status.

The objective of this paper was to analyze the differences of canopy reflectance among erectophile, planophile, and horizontal LAD varieties, and to develop an approach to distinguish these different LAD varieties using two-temporal and bidirectional canopy-reflected spectrum.

II. MATERIALS AND EXPERIMENTS

A. Experimental Design

The experiments were carried out at China National Experimental Station for Precision Agriculture, which is located in Changping District, Beijing (40°11'N, 116°27'E), China, in 2003 and 2004. The nutrient contents of soil (0–0.20 m) were as follows: 14.2–14.8 g · kg⁻¹ of organic material; 0.81–1.00 g · kg⁻¹ of total nitrogen; 20.1–55.4 mg · kg⁻¹ of available phosphorus; and 117.6–129.1 mg · kg⁻¹ of available potassium. The organic matter was measured by the Walkley–Black acid digestion method [30]. A total of N contents were determined after digestion with H₂SO₄, NaOH, and K₂SO₄ with the Kjeldahl method [2]. The B-339 Distillation Unit (BÜCHI Analytical Ltd., Flawil, Switzerland) was used for N -content analysis. The available phosphorus content in soil samples was determined by the Olsen method, after it had been extracted with 0.5-M NaHCO₃ [20]. The available potassium was determined by using the 1-M NH₄OAc extraction method [1], and soil extracts were analyzed by flame spectrometry, which determined the potassium content.

Crop canopy geometry was classified by mean LAD (MLAD). The wheat varieties with $90^\circ \geq \text{MLAD} \geq 65^\circ$ were treated as erectophile LAD varieties, with $40^\circ < \text{MLAD} < 65^\circ$ as planophile LAD varieties, and with $0 \leq \text{MLAD} \leq 40^\circ$ as horizontal LAD varieties. In 2003, 18 winter wheat varieties were investigated: six erectophile LAD varieties (Lumai21 (LM21), Jing411 (J411), P7, Laizhou3279 (LZ3279), Nongda3291 (ND3291), and I-93); six planophile LAD varieties [Jingwang10 (JW10), 6211, CA16, 95128, Jingdong8 (JD8), Chaoyou66 (CY66)]; and six horizontal LAD varieties [Zhongyou 9507 (ZY9507), Jing 9428 (J9428), 4P3, Linkang2 (LK2), Nongda 3214 (ND3214), and Zhongmai 16 (ZM16)].

In 2004, 12 winter wheat varieties were investigated at the same experimental base as in 2003: six erectophile LAD varieties (I-93, J411, LZ3279, LM21, ND3291, and P7) and six horizontal LAD varieties (4P3, ZM16, J9428, ZY9507, LK2, and ND3214).

B. Data Acquisition

1) *In Situ Canopy-Reflected Spectrum*: For each LAD variety, three samples were measured. A 1 × 1 m area of each sample was selected to measure the canopy reflectance and to analyze the biophysical and biochemical crop canopy features. Canopy reflectance was measured at a height of 1.3 m under clear sky conditions between 10:00 and 14:00, using an ASD FieldSpec Pro spectrometer (Analytical Spectral Devices, Boulder, CO) fitted with a 25° field-of-view fiber optic adaptor and operated in the 350–2500-nm spectral range. A 0.4 m × 0.4 m BaSO₄ calibration panel was used for calculating the black and baseline reflectance. Vegetation reflectance measurements were taken by averaging 20 scans at optimized integration times. Calibration panel reflectance measurements were taken before and after the vegetation measurements.

2) *Canopy BRDF Reflected Spectrum*: Canopy BRDF reflectance was measured by using the same spectrum instrument as that in measuring the *in situ* canopy-reflected spectrum. The instrument was fixed on rotating bracket multiangular viewing equipment (Fig. 1), which enables BRDF observation of the same object in a short time. The multiangular viewing equipment was also used by Yan *et al.* [32] for the bidirectional canopy thermal-infrared (TIR) temperature measurement. The observation plane was the principal plane and the cross-principal plane. The view zenith changes from 0° to 65° at intervals of 5°.

3) *Airborne Multiangle TIR/VNIR Imaging System (AMTIS) Hyperspectral Images*: Airborne hyperspectral images of the field exercise were acquired in year 2004 by using the AMTIS, which was designed by the Chinese Academy of Science (CAS). The AMTIS consists of a charge-coupled device (CCD) camera for visible band (VIS, 400–700 nm), a CCD camera for near-infrared band (NIR, 700–900 nm), and a thermal camera (TIR, 7500–13000 nm) with 1024 × 1024 elements. It has a field view of 30° and is capable of acquiring images of 2 m with VIR or NIR, and 5.0 m with TIR spatial resolution at a flying altitude of 4000 m above the ground. The AMTIS has a wavelength range of 400–850 nm with a spectral resolution of 5 nm. It can view the surface at a number of view angles, providing the potential for retrieval of bidirectional land surface reflectance. It is capable of continuously imaging the surface at nine fixed viewing angles ($\pm 45^\circ$, $\pm 33.75^\circ$, $\pm 22.5^\circ$, $\pm 11.25^\circ$, and nadir).

4) *Leaf Area Index (LAI)*: All the plants of 0.6 m × 0.6 m area were harvested immediately after the spectral measurements, and the LAD parameters were measured. The samples were placed in a cooled black plastic bag and transported to the laboratory for subsequent analysis. Leaves of all the sampled plants were collected together to determine the LAI.

A subsample of plant leaves was used to measure the leaf area in the lab with a Li-Cor 3100 area meter. The leaf area of

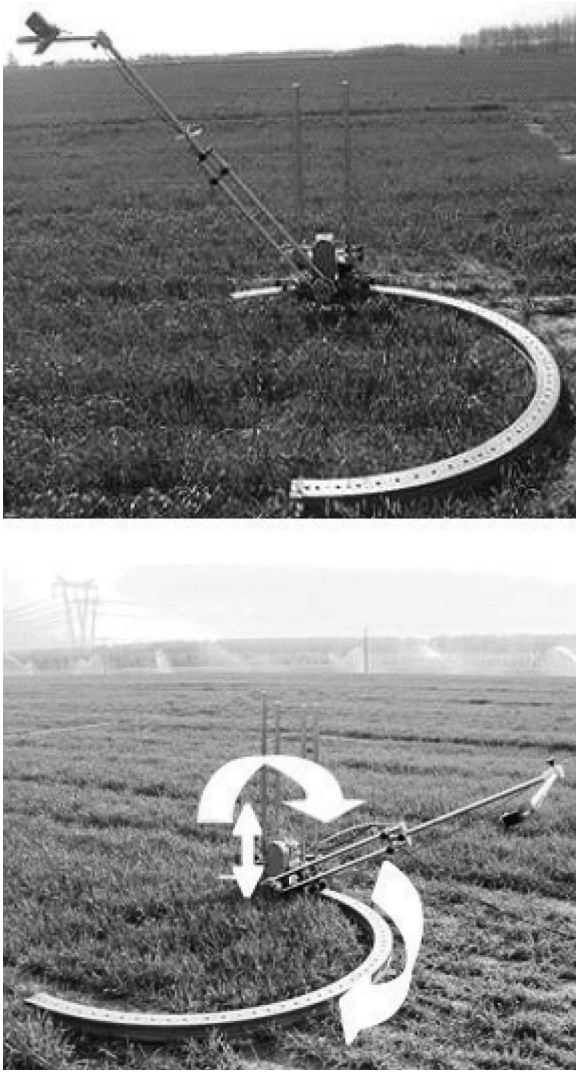


Fig. 1. Rotating bracket for observing BRDF canopy reflectance.

the subsample (LA_{sub}) was used to establish the LAI of the $0.6\text{ m} \times 0.6\text{ m}$ sample area with the following equation. This equation was also used by Liu *et al.* [17]:

$$LAI = \left[LA_{sub} \times \frac{\text{total leaves' weight}}{\text{subsample leaves' weight}} \right] \div [\text{sampled projection area}]. \quad (1)$$

III. METHODS AND RESULTS

A. Effect of Crop LAD on Canopy-Reflected Spectrum

The effects of LAI and crop LAD on canopy reflectance were studied among erectophile, planophile, and horizontal LAD varieties. We studied the canopy-reflected spectrum at the 450-nm (blue), 550-nm (green), 680-nm (red), 800-nm, and 1100-nm bands (NIR). The most common vegetation index was the normalized difference vegetation index (NDVI). It was defined by Rouse *et al.* [24] as follows:

$$NDVI = (NIR - R)/(NIR + R). \quad (2)$$

TABLE I
REFLECTED SPECTRUM AND NDVI FOR DIFFERENT LAD VARIETIES UNDER DIFFERENT LAI

Mean LAI	Crop geometry	Variety	LAI	450 nm	550 nm	680 nm	800 nm	1100 nm	NDVI
LAI≈2.3	ELT	LM21	2.38	2.32	4.69	3.67	30.40	32.84	0.78
		PLT	9158	2.34	2.51	5.32	2.83	37.68	38.80
	HLT	LK2	2.20	2.57	5.29	3.01	39.83	41.84	0.86
		STDEV	0.09	0.13	0.36	0.44	4.94	4.58	0.04
		VAR	0.01	0.02	0.13	0.19	24.41	20.93	0.00
		MV	2.31	2.47	5.10	3.17	35.97	37.83	0.83
CV	4.10	5.16	7.02	13.92	13.74	12.09	5.20		
LAI≈2.6	ELT	P7	2.59	2.28	4.53	3.02	34.13	35.95	0.84
		PLT	ZM16	2.59	2.40	4.79	3.04	38.32	40.42
	HLT	ZY9507	2.53	2.73	6.11	3.52	41.18	43.81	0.88
		STDEV	0.03	0.24	0.85	0.28	3.55	3.94	0.02
		VAR	0.00	0.06	0.71	0.08	12.59	15.55	0.00
		MV	2.57	2.47	5.14	3.19	37.88	40.06	0.86
CV	1.35	9.55	16.43	8.69	9.37	9.84	2.70		
LAI≈3.1	ELT	I-93	3.07	1.80	3.88	2.06	35.08	35.84	0.86
		PLT	CY66	3.11	2.33	4.78	2.84	36.11	38.02
	HLT	ND3214	3.15	2.30	5.20	2.71	40.23	42.11	0.90
		STDEV	0.04	0.30	0.67	0.42	2.72	3.18	0.02
		VAR	0.00	0.09	0.45	0.17	7.41	10.11	0.00
		MV	3.11	2.14	4.62	2.54	37.14	38.66	0.87
CV	1.29	13.98	14.56	16.39	7.33	8.22	1.99		
LAI≈4.1	ELT	J411	4.42	1.72	3.91	1.69	42.75	42.35	0.89
		PLT	JD8	4.14	2.25	4.86	2.27	43.59	44.75
	HLT	4P3	4.10	2.50	5.44	2.61	47.05	47.34	0.91
		STDEV	0.06	0.40	0.77	0.46	2.28	2.50	0.01
		VAR	0.00	0.16	0.59	0.22	5.20	6.24	0.00
		MV	4.15	2.16	4.74	2.19	44.46	44.81	0.90
CV	1.47	18.44	16.24	21.23	5.13	5.58	0.78		

Note:

1. ELT: Erectophile LAD varieties; PLT: Planophile LAD varieties; HLT: Horizontal LAD varieties
2. STDEV: Standard deviation; VAR: Variance; CV: Coefficient of Variation; MV: Mean value

In this paper, 800 nm at near infrared (NIR) and 680 nm at red (R) were chosen. These bands and the resulting NDVI could be used to evaluate the crop-growth status and to distinguish different LAD varieties.

The canopy reflectance (in percent) at 450, 550, 680, 800, and 1100 nm, and the NDVI value for different LAD varieties were different at the different approximate LAI values (Table I). The coefficient of variation (CV) of the canopy reflectance among erectophile, planophile, and horizontal LAD varieties at near-infrared band and NDVI values gradually decreased as the LAI value increased. This might mean that when LAI was large, there was less effect of LAD in the radiation and transmission (RT) regime; the difference of canopy reflectance for different LAD varieties reduced as the LAI value increased; and the NDVI value was likely to be saturated as the LAI value was more than four. Crop LAD identification should be made at the proper (not very small and not very large) LAI growth stage. It was mentioned that the elongation stage (LAI was about 2–3) could be used for wheat LAD identification.

B. Identifying Crop LAD Using Two-Temporal Canopy Reflectance

The canopy spectral reflectance of 800 nm (in percent format) at erecting stage [R800(B)] indicated the crop

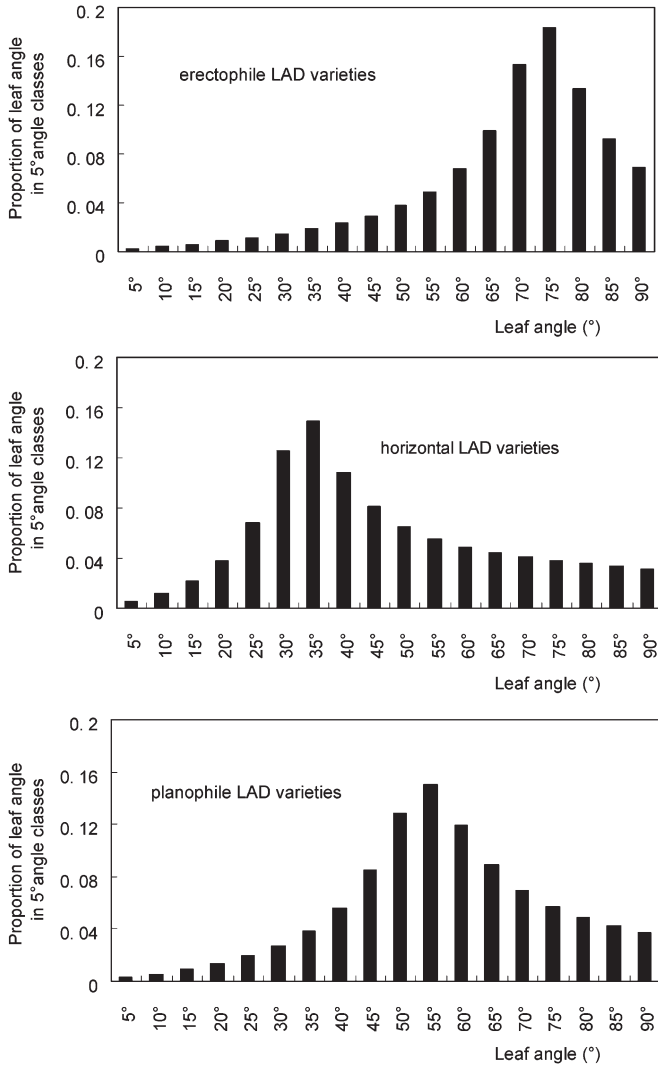


Fig. 2. Frequency distributions of leaf angle in 5° angle classes for erectophile, planophile, and horizontal varieties. Note: Leaf angle is measured as the angle from the horizontal (0—flat; 90—vertical/steep).

sowing-density information, and the canopy spectral reflectance of 800 nm at elongation stage [R800(A)] indicated the crop sowing-density information and the increment from erecting stage to elongation stage. The distribution features of canopy reflectance at the different stages are shown in two-dimensional spectral (x axis) and spectral-ratio (y axis) coordinate space (Fig. 2). The horizontal LAD varieties are mainly located in the upper part of the coordinate system, while the erectophile LAD varieties are mainly located in the lower part. The reason may be that the soil has effects more on the canopy spectral reflectance of the erectophile LAD varieties at erecting stage than that of the horizontal LAD varieties due to the difference of ground covered percentage by wheat canopy (the between-row spaces were not fully covered by wheat plants). The horizontal LAD varieties occupied vegetation ground cover percentage quickly after erecting stage. The increment of horizontal LAD varieties was more than that of erectophile LAD varieties because the covering percentage of horizontal LAD varieties was more than that of erectophile LAD varieties at the same

TABLE II
MLA AND ECCENTRIC RATE FOR DIFFERENT LAD VARIETIES

Item	Erectophile varieties	Planophile varieties	Horizontal varieties
Mean leaf angle(°)	73.8	53.5	32.7
Eccentric rate	0.9945	0.9927	0.9956

LAI conditions. The ratio of R800(A) to R800(B) indicates the information of the increment from erecting stage to elongation stage, and it also could eliminate the difference of the sowing densities for different LAD varieties.

The ratio of R800(A) to R800(B) of horizontal LAD varieties exceeded 1.6, and that of planophile LAD varieties was between 1.4 and 1.6. The ratio of planophile exceeded the ratio of horizontal LAD varieties by 25%. In contrast, the ratio of R800(A) to R800(B) of erectophile LAD varieties did not exceed 1.4. Hence, the different LAD varieties could be identified by using the spatial distribution features in the coordinate system developed with two-temporal spectral and spectral-ratio data. The spatial distribution features in a controlled coordinate system can then be applied to classify the crop LAD. We can use the two-temporal space-borne satellite data at the elongation stage (A) and the erecting stage (B) for the crop LAD identification.

C. LAD by Beta-Distribution Function and Radiative Transfer SAILTH Model

The LAD distributions can also be expressed by using the beta distribution [8]. Frequency distributions of leaf angle for erectophile, planophile, and horizontal varieties are shown in Table II. The mean leaf angle (MLA) for erectophile varieties is 73.8°, while that of planophile varieties is 53.5°, and that of horizontal varieties is 32.7°. The MLA for erectophile varieties is 73.8°, while that of planophile varieties is 53.5°, and that of horizontal varieties is 32.7°. The eccentric rate for erectophile varieties is 0.9945, while that of planophile varieties is 0.9927, and that of horizontal varieties is 0.9956. The proportion of leaf angle in 5° angle classes (from 5° to 90°) for erectophile varieties is dominated by about 75°, while that of planophile varieties is dominated by about 55°, and that of horizontal varieties is dominated by about 35° (Fig. 3).

D. Identifying Crop LAD by Bidirectional Canopy Reflectance

We identify crop LAD using bidirectional canopy reflectance to retrieve physical parameters with a semiempirical BRDF model. It can be expressed with a linear equation [25]

$$R(\theta_i, \theta_v, \varphi) = f_{iso} + f_{vol}k_{vol}(\theta_i, \theta_v, \varphi) + f_{geo}k_{geo}(\theta_i, \theta_v, \varphi) \tag{3}$$

where k_{vol} is a function of view zenith θ_v and illumination zenith θ_i ; relative azimuth φ describes the volume scattering

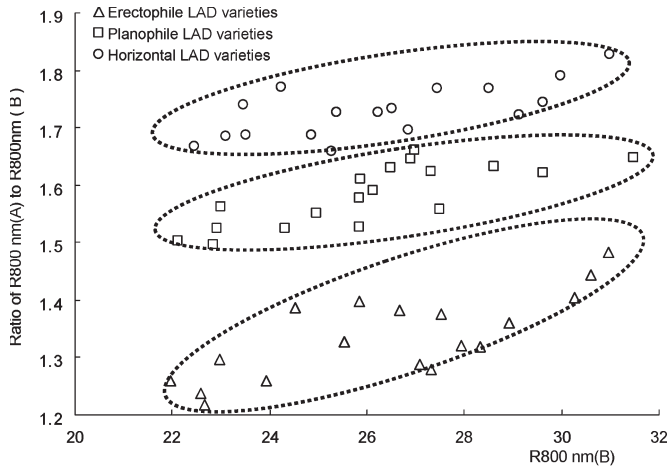


Fig. 3. Response of canopy reflectance (percent) and ratio of 800 nm for different LAD varieties at erecting and elongation stage in year 2003. Note: 1) R800 nm (B) was the canopy reflectance of 800 nm at erecting stage; R800 nm (A) was the canopy reflectance of 800 nm at elongation stage. 2) The ratio of R800(A) to R800(B) was shown on the abscissa axis, and R800(B) was shown on the ordinate axis.

from canopy; and k_{geo} describes the surface scattering from the canopy. These functions are, respectively, called volumetric and geometric kernels. In (4), f_{vol} and f_{geo} are, respectively, the weights for the volumetric and geometric kernels. f_{iso} is a constant corresponding to the isotropic reflectance. Through matrix inversion with multiangle reflectance data by setting the derivative of the error function to zero, we can obtain the parameters f_{iso} , f_{vol} , and f_{geo} . The problem in using kernel weights is that the volumetric and geometric effects are not mutually exclusive, where the retrieved weights do not have a direct relationship with the measurable biophysical parameters, such as LAI. By combining the weights of the red and near-infrared bands, our model can obtain structural information by retrieving biophysical parameters from the physical BRDF model and a number of bidirectional observations [13].

Gao *et al.* [6] calculated SSI as follows:

$$\text{SSI} = \ln \left(f_{\text{vol}}^{\text{nir}} / f_{\text{geo}}^{\text{red}} \right) \quad (4)$$

where $f_{\text{vol}}^{\text{nir}}$ is the volumetric kernel weight at the near-infrared band, and $f_{\text{geo}}^{\text{red}}$ is the geometric kernel weight at the red spectral band.

d'Entremont *et al.* [4] proposed the normalized difference f-index (NDFI), which was based on the normalized difference of f_{vol} and f_{geo} as follows:

$$\text{NDFI} = \frac{f_{\text{vol}} - f_{\text{geo}}}{f_{\text{vol}} + f_{\text{geo}}}. \quad (5)$$

In this paper, the structural parameter-sensitive index (SPEI) is defined for crop LAD identification, which was based on the weight of near-infrared band for the volumetric kernel ($f_{\text{vol}}^{\text{nir}}$), the weight of red band for the geometric kernel ($f_{\text{geo}}^{\text{red}}$), and the



Fig. 4. Different crop LAD variety fields located in the AMTIS image.

weight of near-infrared band for the constant corresponding to isotropic reflectance ($f_{\text{iso}}^{\text{nir}}$) as follows:

$$\text{SPEI} = \text{OA} / \text{OAL}$$

$$\text{OA} = f_{\text{vol}}^{\text{nir}} - \frac{f_{\text{iso}}^{\text{nir}}}{10} - f_{\text{geo}}^{\text{red}}$$

$$\text{OAL} = f_{\text{vol}}^{\text{nir}} + \frac{f_{\text{iso}}^{\text{nir}}}{10} - f_{\text{geo}}^{\text{red}}. \quad (6)$$

For the vegetation canopy, the high leaf transmittance observation in the near-infrared band results in high multiple scattering within the canopy and decreases the reflectance anisotropy. The features of LAI are therefore best described by nadir $f_{\text{iso}}^{\text{nir}}$, while the features of LAI and leaf LAD are best described by nadir $f_{\text{vol}}^{\text{nir}}$, and soil information is best described by nadir $f_{\text{geo}}^{\text{red}}$. The value of OA indicated the crop LAD and leaf-LAD information, and the value of OAL indicated the crop LAD, leaf-LAD, and LAI information. By reasonably combining the $f_{\text{vol}}^{\text{nir}}$, $f_{\text{iso}}^{\text{nir}}$, and $f_{\text{geo}}^{\text{red}}$ kernels' weights, we can detect the differences of crop LAD.

The LAI value of horizontal LAD varieties (e.g., ZY9507) is 3.5 and that of erectophile LAD varieties (e.g., J411) is 3.8, which had almost the same LAI value (Fig. 4). The observation conditions for ZY9507 and J411 are described in Table III. The data are used for the semiempirical-BRDF-model parameter inversion observed for four times at different solar azimuth angles and different observation azimuth angles. The inversion result of kernel parameters for erectophile LAD variety J411 and horizontal LAD variety ZY9507 is shown in Table IV. The value of f_{iso} between different crop LAD varieties is similar, but the value of f_{vol} and f_{geo} between different crop LAD varieties was different. The value of f_{vol} for ZY9507 is more than that of J411 at the visible and near-infrared bands, and the value of f_{geo} for ZY9507 is less than that of J411 at the visible and near-infrared bands. This phenomenon is caused by the ground covering percentages difference caused by LAD, because the horizontal LAD variety ZY9507 has more ground

TABLE III
DESCRIPTION OF OBSERVATION CONDITIONS FOR DIFFERENT LAD VARIETIES AT ERECTING STAGE (ON APRIL 17, 2005)

Parameters		Horizontal LAD variety (ZY9507) on VZA				Erectophile LAD variety (J411) on VZA			
LAI		3.50				3.80			
Observation times	The first time	The second time	The third time	The fourth time	The first time	The second time	The third time	The fourth time	
Beijing local time(h:m)	09:40	11:00	14:30	15:40	10:20	11:50	15:00	16:00	
SZA	45.175	33.158	41.877	53.293	38.637	29.818	46.787	58.432	
SAA	119.523	147.464	234.991	251.152	131.508	168.231	242.863	256.676	
	BW	119.523	147.464	234.991	251.152	131.508	168.231	242.863	256.676
OAA	FW	299.523	327.464	54.991	71.152	311.508	348.231	62.863	76.676
	VZA	0-65	0-65	0-65	0-65	0-65	0-65	0-65	0-65

Note: 1. VZA—View zenith angle on the principal plane (°); 2. SZA—Solar zenith angle; 3. SAA—Solar azimuth angle; 4. OAA—Observation azimuth angle; 5. BW—Backward observation; 6. FW—Forward observation

TABLE IV
INVERSION RESULT OF KERNEL PARAMETERS FOR DIFFERENT LAD VARIETIES AT ERECTING STAGE (ON APRIL 17, 2005)

Parameter	Waveband(nm)	Waveband(nm)					
		450	550	680	800	960	1100
Erective leaf type variety (J411)	f_{iso}	0.0332±0.0009	0.0651±0.0013	0.0362±0.0007	0.474±0.012	0.444±0.013	0.480±0.021
	f_{vol}	0.00199±0.00013	0.00820±0.00024	0.00194±0.00031	0.0764±0.0022	0.0572±0.0034	0.0710±0.0028
	f_{geo}	0.0108±0.0007	0.0127±0.0009	0.0130±0.0006	0.0104±0.0011	0.00165±0.00039	0.0110±0.00045
Horizontal leaf type variety (ZY9507)	f_{iso}	0.0323±0.0017	0.0654±0.0012	0.0328±0.0021	0.457±0.025	0.431±0.037	0.465±0.048
	f_{vol}	0.00433±0.00014	0.0152±0.00023	0.00412±0.00018	0.0844±0.0015	0.0825±0.0026	0.0840±0.0035
	f_{geo}	0.00895±0.00015	0.00919±0.00011	0.00912±0.00022	0.00863±0.00006	0.00473±0.00021	0.00776±0.00013

TABLE V
COMPARISON OF SPEI, SSI, AND NDFI INDEXES FOR DIFFERENT LAD VARIETIES

Varieties	Band selection	Value	SPEI	SSI	NDFI
Erect leaf type variety (J411)	Red band 680 nm	The reference value	0.144	1.769	0.709
	Near-infrared band 800 nm				
Erect leaf type variety (J411)	Red band 680 nm	The variable value	0.118	1.695	0.690
	Near-infrared band 1100 nm				
RER			-17.678	-4.180	-2.666
Horizontal leaf type variety (ZY9507)	Red band 680 nm	The variable value	0.244	2.226	0.805
	Near-infrared band 800 nm				
RER			69.814	25.863	13.627
Horizontal leaf type variety (ZY9507)	Red band 680 nm	The variable value	0.233	2.220	0.804
	Near-infrared band 1100 nm				
RER			62.019	25.542	13.486

Note : $RER = \frac{\text{the variable value} - \text{the referenced value}}{\text{the variable value}} \times 100$

covering percentages than erectophile LAD variety J411 under almost the same LAI value [12].

The semiempirical-BRDF-model parameter-inversion results are derived from SPEI, SSI, and NDFI index for different crop LAD varieties (Table V).

The SPEI, SSI, and NDFI indexes for erectophile LAD variety J411 at red band 680 nm and near-infrared band 800 nm are defined as the referenced value. The kernel index for erectophile LAD variety J411 at red band 680 nm and near-infrared band 1100 nm, and that of horizontal LAD variety ZY9507 at red band 680 nm and near-infrared band 800 nm (1100 nm) is defined as the variable value. The RER is defined as

$$RER = \frac{\text{the variable value} - \text{the referenced value}}{\text{the variable value}} \times 100. \quad (7)$$

The RER value of different kernel indexes at different wavebands for the same variety is SPEI > SSI > NDFI. The RER value for different crop LAD is SPEI > SSI > NDFI. As mentioned above, the RER value of the kernel index for crop LAD identification is SPEI > SSI > NDFI under almost the same LAI conditions. SPEI is proved to be more sensitive (the maximal RER value) to identify the crop LAD than SSI and NDFI does. Thus, SPEI can be used to distinguish the different crop LAD varieties.

The different crop LAD varieties are located in the AMTIS images as in Fig. 3. The field of NW1 is cultivated with horizontal LAD varieties ZY9507 and JD8. The NW2 is cultivated

TABLE VI
LAI AND SOWING DATA FOR DIFFERENT VARIETIES
IN THE AMTIS IMAGE

	Variety	North latitude	East longitude	LAI	Sowing date
	J411			2.7	Oct.10,2003
Erective LAD varieties	P7	40°11'39.5"	116°34'20.9"	2.6	Oct.8,2003
	I-93	40°11'39.4"	116°34'35.9"	2.2	Oct.12,2003
	ZY9507			2.5	Oct.9,2003
Horizontal LAD varieties	J9428	40°11'39.2"	116°34'14.6"	2.2	Oct.14,2003
	LK2	40°11'51.8"	116°34'49.4"	1.9	Oct.15,2003

with erectophile LAD varieties J411 and P7. NW3, NW4, and NW5 are cultivated with erectophile LAD varieties I-93 and horizontal LAD varieties LK 2 (Table VI).

The identification of different LAD varieties by the SSI, NDFI, and SPEI spectral indexes is shown in Fig. 5. Mapping the AMTIS image is done by SSI [Fig. 5(a)], by NDFI [Fig. 5(b)], and by SPEI [Fig. 5(c)]. The SSI index can distinguish crops from buildings very well but cannot distinguish different crop LAD varieties. The NDFI index cannot distinguish among crops, buildings, and the different crop LAD varieties. SPEI can distinguish different crop LAD varieties (erectophile and horizontal LAD varieties) very well. Comparing the mapping result by SSI, NDFI, and SPEI for AMTIS image of winter wheat at the erecting stage, SPEI was the best spectral index for crop LAD identification.

IV. DISCUSSION

Because this paper was carried out under almost the same ecological conditions, and because the selected varieties were limited, the results cannot be applied directly to different ecological conditions and other varieties. Studies on how environmental conditions influence the different LAD variety identifications should be carried out later. Our method contributes to developing optimal procedures for identifying different LAD varieties through the analysis of canopy reflectance at 800 nm for large areas at the erecting and elongation stages. With the results of this paper, multiangle spaceborne sensors can be developed with a view angle of 15°, 30°, and 45° at visible and near-infrared bands. Our results allow an on-site and nonsampling mode of crop LAD identification, which is useful in using remote sensing for crop-growth monitoring, fertilizing, and water management without *a priori* knowledge. Moreover, a careful analysis should be carried out to investigate the effects of bandwidth. Further studies are needed to confirm and improve the results mentioned in this paper.

V. CONCLUSION

The canopy reflectance of different LAD varieties has significant differences between their erecting stage and elongation stage. Different LAD varieties have similar canopy reflectance in the red band (680 nm) and near-infrared band (800 nm) at the erecting stage, while they have significant differences at the elongation stage. The canopy reflectance of horizontal LAD varieties was lower than that of erectophile LAD varieties in

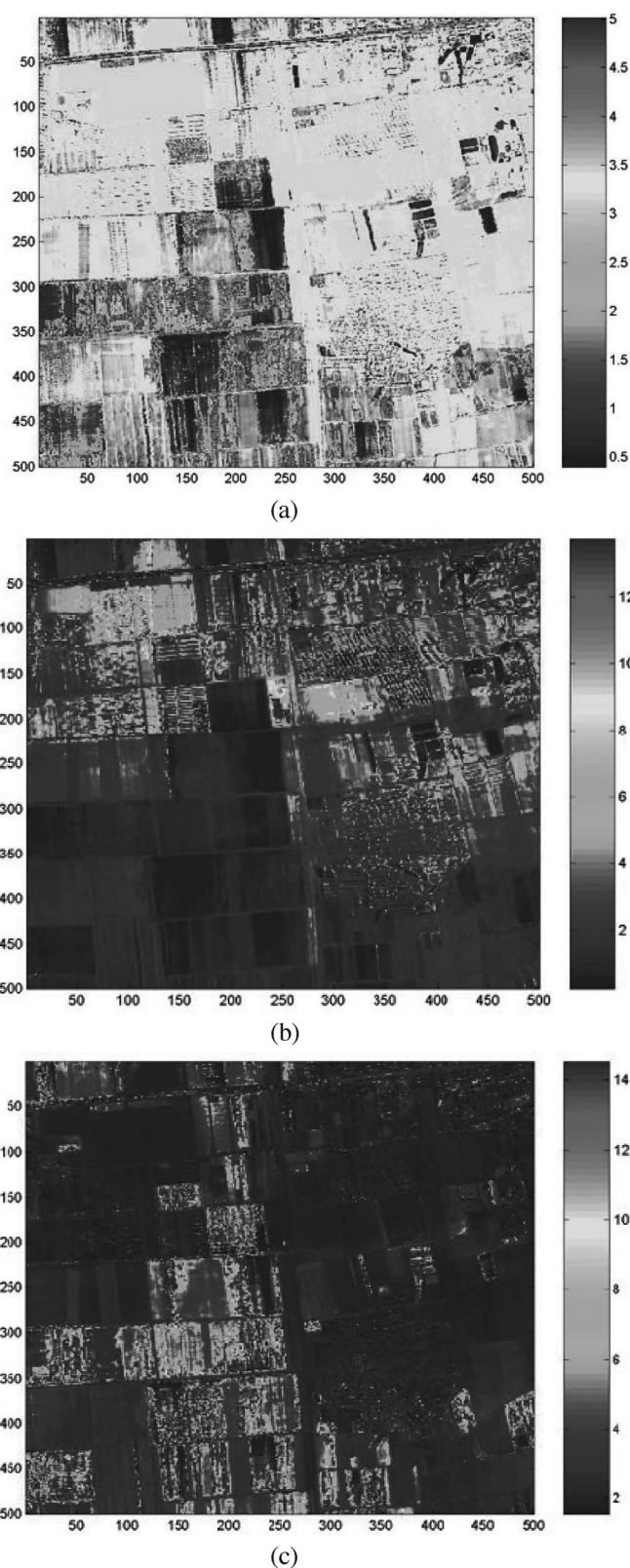


Fig. 5. Identification of different crop LAD varieties by SSI, NDFI, and SPEI spectral indexes in year 2004. (a) Mapping AMTIS image by SSI index. (b) Mapping AMTIS image by NDFI index. (c) Mapping AMTIS image by SPEI index.

the red band, but it is higher than that of the erectophile LAD varieties in the near-infrared band.

The SPEI is proved to be more sensitive to identify erectophile, planophile, and horizontal LAD varieties than the SSI and the NDFI.

ACKNOWLEDGMENT

The authors would like to thank Z. Ma, W. Li, and H. Chang for data collection. They would also like to thank J. Teng, W. Huang, and X. Meng, for their editing, and the three peer reviewers and editors for the improvement of this paper.

REFERENCES

- [1] R. H. Bray, "Soil-plant relations: I. The quantitative relation of exchangeable potassium to crop yield and to crop response to potash additions," *Soil Sci.*, vol. 58, no. 4, pp. 305–324, 1944.
- [2] J. M. Bremner, *Method of Soil Nitrogen Analysis*, Y. C. Cao, Ed. Beijing, China: Agricultural Press, 1981, pp. 208–230.
- [3] R. Bonhome, *Techniques d'Etudes Facteurs Physiques de la Biosphere*. Paris, France: INRA, 1970, pp. 501–505.
- [4] R. P. d'Entremont, C. B. Schaaf, W. Lucht, and A. H. Strahler, "Retrieval of red spectral albedo and bidirectional reflectance using AVHRR HRPT and GOES satellite observations of the New England region," *J. Geophys. Res.*, vol. 104, no. 6, pp. 6229–6239, 1999.
- [5] S. F. Daniel, and W. Mark, "Leaf size and angle vary widely across species: What consequences for light interception?" *New Phytol.*, vol. 158, no. 3, pp. 509–525, Jun. 2003.
- [6] F. Gao, C. B. Schaaf, A. H. Strahler, Y. Jin, and X. W. Li, "Detecting vegetation structure using a kernel-based BRDF model," *Remote Sens. Environ.*, vol. 86, no. 2, pp. 198–205, Jul. 2003.
- [7] D. M. Gates, *Biophysical Ecology*. New York: Springer-Verlag, 1980.
- [8] N. S. Goel and D. Strebel, "Simple beta distribution representation of leaf orientation in vegetation canopies," *Agron. J.*, vol. 76, no. 5, pp. 800–803, 1984.
- [9] F. G. Hall, Y. E. Shimabukuro, and K. E. Huemmrich, "Remote sensing of forest biophysical structure using mixture decomposition and geometric reflectance models," *Ecol. Appl.*, vol. 5, no. 4, pp. 993–1013, Nov. 1995.
- [10] T. Houet, L. Hubert-Moy, G. Mercier, and P. Gouery, "Estimation and monitoring of bare soil/vegetation ratio with SPOT VEGETATION and HRVIR," in *Proc. IGARSS*, 2003, pp. 3248–3250.
- [11] K. Hikosaka and T. Hirose, "Leaf angle as a strategy for light competition—Optimal and evolutionarily stable light-extinction coefficient within a leaf canopy," *Ecoscience*, vol. 4, no. 4, pp. 501–507, 1997.
- [12] W. J. Huang, J. H. Wang, L. Y. Liu, J. D. Wang, C. W. Tan, C. J. Li, A. J. Wang, and X. Y. Song, "Study on identification plant structural types based on multi-temporal and bidirectional canopy spectrum," *Trans. Chinese Soc. Agricultural Eng.*, vol. 21, no. 6, pp. 82–86, 2005. In Chinese.
- [13] D. Kimes, Y. Knjazikhin, J. Privette, A. Abuelgasim, and F. Gao, "Inversion methods for physically based models," *Remote Sens. Rev.*, vol. 18, pp. 381–439, 2000.
- [14] S. K. Li and C. T. Wang, "The methods of obtaining and expressing information of crop plant shape and population structure," *J. Shihezi University (Natural Science)*, vol. 1, no. 3, pp. 250–256, 1997. In Chinese.
- [15] X. W. Li and J. D. Wang, *Optical Remote Sensing Models and Structure Parameterization for Vegetation*. Beijing, China: Science Press, 1995, pp. 103–105.
- [16] X. W. Li and A. H. Strahler, "Geometric-optical modeling of a conifer forest canopy," *IEEE Trans. Geosci. Remote Sens.*, vol. GRS-23, no. 5, pp. 705–721, 1985.
- [17] L. Y. Liu, J. H. Wang, Y. S. Bao, W. J. Huang, Z. Ma, and H. Zhao, "Predicting winter wheat condition, grain yield and protein content using multi-temporal EnviSat-ASAR and Landsat TM satellite images," *Int. J. Remote Sens.*, vol. 27, no. 4, pp. 737–753, Feb. 2006.
- [18] S. M. Mickelson, C. S. Stuber, L. Senior, and S. M. Kaeppler, "Quantitative trait loci controlling leaf and tassel traits in a B73 × Mo17 population of maize," *Crop Sci.*, vol. 42, no. 6, pp. 1902–1909, Nov. 2002.
- [19] S. M. Moran, Y. Inoue, and E. M. Barnes, "Opportunities and limitations for image-based remote sensing and precision crop management," *Remote Sens. Environ.*, vol. 61, no. 3, pp. 319–346, Sep. 1997.
- [20] S. R. Olsen, C. V. Cole, F. S. Watanabe, and L. A. Dean, *Estimation of Available Phosphorus in Soils by Extraction With Sodium Bicarbonate*. Washington, DC: U.S. Gov. Print. Office, 1954. USDA Circ. 939.
- [21] G. E. Pepper, R. B. Pearce, and J. J. Mock, "Leaf orientation distribution and yield of maize," *Crop Sci.*, vol. 17, no. 6, pp. 883–886, 1977.
- [22] D. A. Roberts, S. L. Ustin, S. Ogunjemiyo, J. Greenberg, S. Z. Dobrowski, J. Chen, and T. M. Hinckley, "Scaling up the forests of the Pacific Northwest using remote sensing," *Ecosystems*, vol. 7, no. 5, pp. 545–562, 2004.
- [23] A. Rosema, W. Verhoef, H. Noorbergen, and J. J. Borgesius, "A new forest light interaction model in support of forest monitoring," *Remote Sens. Environ.*, vol. 42, no. 1, pp. 23–41, Oct. 1992.
- [24] J. W. Rouse, R. H. Haas, J. A. Schell, D. W. Deering, and J. C. Harlan, "Monitoring the vernal advancement of retrogradation of natural vegetation," NASA Goddard Space Flight Center, Greenbelt, MD, pp. 152–371, Type III, Final Rep. no. 1, 1974.
- [25] J. L. Roujean, M. Leroy, and P. Y. Deschamps, "A bidirectional reflectance model of the Earth's surface for the correction of remote sensing data," *J. Geophys. Res.*, vol. 97, no. D18, pp. 20455–20468, 1992.
- [26] S. Sandmeier, C. Muller, B. Hosgood, and G. Andreoli, "Physical mechanisms in hyperspectral BRDF data of grass and watercress," *Remote Sens. Environ.*, vol. 66, no. 2, pp. 222–233, Nov. 1998.
- [27] P. J. Sellers, "Canopy reflectance, photosynthesis and transpiration," *Int. J. Remote Sens.*, vol. 6, no. 8, pp. 1335–1372, 1985.
- [28] H. Utsugi, "Angle distribution of foliage in individual *Chamaecyparis obtusa* canopies and effect of angle on diffuse light penetration," *Trees Struct. Function*, vol. 14, no. 1, pp. 1–9, 1999.
- [29] K. S. Verma, R. K. Saxena, T. N. Hajare, and S. C. Ramesh, "Gram yield estimation through SVI under variable soil and management conditions," *Int. J. Remote Sens.*, vol. 19, no. 13, pp. 2469–2476, 1998.
- [30] A. Walkley and I. A. Black, "An examination of Degtjareff method for determining soil organic matter and a proposed modification of the chromic acid titration method," *Soil Sci.*, vol. 37, no. 1, pp. 29–38, 1934.
- [31] G. J. Yan, J. Wu, J. D. Wang, C. G. Zhu, and X. W. Li, "Spectral prior knowledge and its use in the remote sensing based inversion of vegetation structure," *J. Remote Sens.*, vol. 6, no. 1, pp. 1–6, 2002.
- [32] G. J. Yan, L. M. Jiang, J. D. Wang, L. F. Chen, and X. W. Li, "Thermal bidirectional gap probability model for row crop canopies and validation," *Sci. China, Ser. D*, vol. 46, no. 12, pp. 1241–1249, 2003.
- [33] J. H. Zhang, K. Wang, J. S. Bailey, and R. C. Wang, "Predicting nitrogen status of rice using multispectral data at canopy scale," *Pedosphere*, vol. 16, no. 1, pp. 108–117, 2006.



Wenjiang Huang received the Ph.D. degree in cartology and geographical information systems from Beijing Normal University, Beijing, China, in 2005.

Since 2005, he has been a Postdoctoral Research Associate with the Institute of Remote Sensing Applications, Chinese Academy of Science, Beijing. He is also currently an Associate Scientist with the National Engineering Research Center for Information Technology in Agriculture, Beijing. His research interests are quantitative remote sensing and precision farming.



Zheng Niu received the Ph.D. degree in cartology and geographical information systems from the Chinese Academy of Science (CAS), Beijing, in 1996.

He is currently a Senior Scientist with the Institute of Remote Sensing Applications, CAS. His research interests are global-change remote sensing.



Jihua Wang received the Ph.D. degree in agronomy from China Agricultural University, Beijing, in 1995.

From 1996 to 1998, he was a Postdoctoral Research Associate with the International Natural Farming Research Center, Nagano, Japan. He is currently a Senior Scientist and Vice Director of the National Engineering Research Center for Information Technology in Agriculture, Beijing. His research interests are crop physiology and application of remote sensing in agriculture.



Liangyun Liu received the Ph.D. degree in optics from the Xi'an Institute of Optics and Precision Mechanics, Chinese Academy of Science (CAS), Beijing, in 2000.

From 2001 to 2002, he was a Postdoctoral Research Associate with the Institute of Remote Sensing Applications, CAS. He is currently an Associate Scientist with the National Engineering Research Center for Information Technology in Agriculture, Beijing. His research interests are optical sensor and remote-sensing applications.



Qiang Liu received the B.S. degree in computational mathematics from Beijing University, Beijing, China, in 1997 and the Ph.D. degree in cartography and remote sensing from the Institute of Remote Sensing Applications, Chinese Academy of Sciences, Beijing, in 2002.

He is currently an Associate Scientist with the Institute of Remote Sensing Applications, Chinese Academy of Sciences. His main research interest is multiangular remote-sensing modeling and inversion, with applications in agriculture, ecosystems, and forest and urban studies.



Chunjiang Zhao received the Ph.D. degree in agronomy from China Agricultural University, Beijing, in 1991.

He is currently a Senior Scientist and Director of National Engineering Research Center for Information Technology in Agriculture, Beijing. His research interests are precision farming, intelligent information technology in agriculture, and crop decision support systems.

Dr. Zhao received the Excellent Scientist Award by the Ministry of Science and Technology of China in 2001.